Hindered mobility of a particle near a soft interface

Thomas Bickel*
CPMOH, Université Bordeaux 1 & CNRS (UMR 5798), 351 cours de la Libération, 33405 Talence, France
(Received 26 October 2006; published 13 April 2007)

The translational motion of a solid sphere near a deformable fluid interface is studied in the low Reynolds number regime. In this problem, the fluid flow driven by the sphere is dynamically coupled to the instantaneous conformation of the interface. Using a two-dimensional Fourier transform technique, we are able to account for the multiple backflows scattered from the interface. The correction to the mobility tensor is then obtained from the matrix elements of the relevant Green's function. Our perturbative analysis allows us to express the explicit position and frequency dependence of the mobility for small particles. We recover in the steady limit the result for a sphere near a perfectly flat interface. At intermediate time scales, the mobility exhibits an imaginary part which is a signature of the elastic response of the interface. In the short time limit, we find that the perpendicular mobility may, under some circumstances, become lower than the bulk value. All the results can be explained using the definition of the relaxation time of the soft interface.

DOI: 10.1103/PhysRevE.75.041403 PACS number(s): 82.70.Dd, 68.05.−n, 47.15.G−

I. INTRODUCTION

The motion of a particle in the vicinity of a bounding surface is a long standing problem in colloidal science [1]. When a colloidal sphere suspended in a quiescent fluid approaches a wall, the drag force acting on it increases with respect to the drag force when far from the wall. This property is attributed to hydrodynamic interactions that develop because of the boundary conditions imposed by the wall on the fluid flow. In addition, the motion of the particle becomes anisotropic since the mobility is higher in the direction parallel to the wall than in the perpendicular direction.

Although the first investigations on the influence of a bounding wall date back to the early work of Lorentz [2], this field has known a certain revival during the past two decades. The main reason for this is certainly the achievement of technical progress, in particular in the field of single-molecule techniques, which allows measurement nowadays of the position-dependent mobility of individual micrometer-size particles with great accuracy. Among the most efficient tools, one can quote the evanescent wave techniques [3,4], single-particle tracking by videomicroscopy [5], particle handling with optical tweezers [6–8], atomic force microscope noise analysis [9], or fluorescent correlation spectroscopy [10]. Those various methods share the common feature of probing the random motion of Brownian objects near one or two solid walls. The mobility coefficients deduced from the experimental data agree remarkably well with theoretical predictions [1].

The renewal of interest in this question is also due to the development of microfluidics [11]. Indeed, by reducing the size of the systems, the influence of surface effects is inevitably enhanced with respect to bulk properties. Consequently, most of the physical phenomena take place near the boundaries. A fundamental understanding of how surface properties might affect the overall flow field has therefore become crucial in order to propose new solutions that would take advantage of this predominance. Lastly, colloidal particles have been suggested recently as local probes of the flow properties near surfaces. This idea has been introduced in the context of the no-slip boundary condition [12], where the motion of the particles is expected to contain a signature of the slip length [10,13]. More generally, one can think of a Brownian particle as a probe of the viscoelastic properties of the bounding surface.

From a theoretical viewpoint, the motion of a solid particle in the presence of a nearby plane interface has been extensively studied in the past. During the last few years, calculations of mobility coefficients have been extended to particles near surfactant-covered interfaces [14], in a liquid film between two fluids [15], or in a Poiseuille flow between planar walls [16]. The effect of fluid inertia has also been accounted for [17], as well as the possibility of liquid slippage at the wall [13]. Here, we reexamine this question for a particle near a fluid-fluid interface. Perturbative results are available for the drag force acting on a small sphere of radius a moving at a distance z_0 of a perfectly flat interface, up to second order in the small parameter a/z_0 [18]. While this problem is of some intrinsic interest, and is a logical starting point in the limit of very high surface tension, it is obvious that a real interface will generally deform owing to the motion of the particle. For finite surface tension, the motion of the particle is expected to be dynamically coupled to the conformations of the interface. Indeed, the fluid flow caused by the displacement of the particle exerts stresses that deform the interface. Relaxing back to its equilibrium position, the interface creates a backflow that in turn perturbs the motion of the particle, and so on. The delay in the response of the soft surface to hydrodynamic stresses is therefore expected to induce memory effects in the motion of the particle [19].

In general, the problem of the motion near a soft surface is highly nonlinear due to the fact that the shape of the interface is unknown. Although it cannot be solved exactly, iterative solutions have been derived when the deformation of the interface is asymptotically small [20,21]. The idea is to first solve the motion of a spherical bead near a flat surface. As the resulting velocity produces an imbalance of normal

*Electronic address: th.bickel@cpmoh.u-bordeaux1.fr

stress at the interface, it is then possible to determine a first nonzero approximation for the deformation [20]. This strategy is, however, limited as it describes only the first "image" correction to hydrodynamic interactions. Also, it assumes a quasi-steady deformation profile and does not allow for a possible delay inherent in the response of an elastic interface.

In this paper, we present an analytical method that rigorously accounts for the infinite series of hydrodynamic reflections on the soft interface. This scheme is achieved within the only assumption that interface deformations remain moderate. The analysis extends a recent study of the author on fluid membranes to more general liquid-liquid interfaces [19]. Although both questions share some similarities, the relaxation dynamics of liquid interfaces differs from that of fluid membranes. Also, the issue of a liquid interface is more involved because of the additional conditions that have to be enforced at the boundary. The aim of this paper is to present a detailed study of the hydrodynamic coupling between the particle and the conformations of the interface. The remaining of the paper is organized as follows. In Sec. II, we specify the system and introduce the general set of equations that govern the problem. Results for the Green's function and the mobility coefficients are then discussed in Sec. III. In particular, it is found that the frequency-dependent mobility switches between two regimes over a time scale corresponding to the relaxation time of the interface. Finally, we come back to the relationship with experiments and draw some concluding remarks in Sec. IV, the details of the calculations being kept for the Appendixes.

II. FORMULATION OF THE PROBLEM

A. Linear hydrodynamics

We consider a spherical particle of radius a moving near a fluid interface in the low Reynolds number regime. The interface separates two viscous, incompressible, and immiscible fluids. Its average position is chosen to coincide with the x-y plane, with the z coordinate directed perpendicular to it. The two fluids are labeled with indices 1 and 2, fluid 1 lying above fluid 2. Furthermore, we denote by η_1 and η_2 the shear viscosities, by ρ_1 and ρ_2 the mass densities, and by $\Delta\rho=\rho_2-\rho_1>0$ the mass density difference. In order to get the mobility tensor of the particle, we shall first evaluate the appropriate Green's function and investigate the effect of a time-dependent point force $\mathbf{F}(t)$ acting at position $\mathbf{r}_0=(x_0,y_0,z_0)$ on the flow field [22]. Without loss of generality, we can assume that the sphere is fully immersed in fluid 1. For small-amplitude and low-frequency motion, the flow velocity $\mathbf{v}(\mathbf{r},t)$ and the pressure $p(\mathbf{r},t)$ are governed by the Stokes equations

$$\eta_\alpha \nabla^2 \mathbf{v} - \boldsymbol{\nabla} p + \mathbf{F}\,\delta(\mathbf{r}-\mathbf{r}_0) = \mathbf{0}, \tag{1}$$

$$\boldsymbol{\nabla}\cdot\mathbf{v} = 0, \tag{2}$$

with $\alpha=1$ or 2, depending on whether the point $\mathbf{r}$ is located above or below the interface. In Eq. (1), δ stands for the Dirac delta function. The two fluids are assumed to be quiescent except for the disturbance flow caused by the motion of the sphere.

B. Physics of interfaces

The Stokes equations have to be solved together with the usual boundary conditions at the interface, namely, the velocity and the tangential constraints must be continuous. The normal-normal component of the stress tensor presents a discontinuity which is balanced by the restoring force exerted by the deformed interface on the fluid (i.e., the Laplace pressure). This question is quite involved since, in principle, the tangential and normal directions depend on the local and instantaneous conformation of the interface. However, an approximate solution can be found for moderate deformations. In this case, the position of the almost flat interface can be described by a single-valued function $h(\boldsymbol{\rho},t)$, with $\boldsymbol{\rho}=(x,y)$. For our purpose, it is more convenient to use the two-dimensional Fourier representation

$$h(\mathbf{q},t) = \int d^2\boldsymbol{\rho}\,\exp[-i\mathbf{q}\cdot\boldsymbol{\rho}]h(\boldsymbol{\rho},t), \tag{3}$$

with $\mathbf{q}=(q_x,q_y)$. The elastic properties of the interface are then described by the Hamiltonian [23]

$$\mathcal{H} = \frac{\gamma}{2}\int d^2\mathbf{q}(q^2+l_c^{-2})|h(\mathbf{q},t)|^2, \tag{4}$$

where γ is the surface tension and $l_c=\sqrt{\gamma/(g\Delta\rho)}$ the capillary length, g being the gravitational acceleration. The capillary length typically lies in the millimeter range for $\gamma\approx 100$ mN/m, but can be as low as a few micrometers for ultrasoft interfaces with $\gamma\approx 0.1$ μN/m [24]. We then proceed in the same manner as for the linearized theory of capillary waves and express all the boundary conditions at the undisplaced interface $z=0$. This hypothesis of smooth deformation is valid up to linear order in the deformation field h, so that our approach is fully consistent with the harmonic description of the interface energy Eq. (4).

C. Method of solution

In spite of these classical simplifications, the coupling between the motion of the particle and the capillary waves leads to a rich behavior. Before solving the Stokes equations, we first remark that the shape of the interface depends on the detailed history of the motion of the particle as well as on the shape at some earlier times. We are then naturally led to perform a Fourier mode analysis in time, the Fourier transform $\tilde{f}(\omega)$ of an arbitrary function $f(t)$ being defined as

$$\tilde{f}(\omega) = \int_{-\infty}^{+\infty} dt\,\exp(-i\omega t)f(t). \tag{5}$$

In addition, one can note that the problem is translationally invariant along the direction parallel to the surface. It is thus helpful to use the two-dimensional Fourier representation introduced above in Eq. (3) [1,25]. It also appears judicious for this study to define a new orthogonal coordinate system that would account for the symmetries of the system. To this aim, the vector fields are decomposed into their longitudinal, transverse, and normal components [16,26,27]. This defines a new set of orthogonal unit vectors $(\hat{\mathbf{q}},\hat{\mathbf{t}},\hat{\mathbf{n}})$, where $\hat{\mathbf{q}}$ is the

unit vector parallel to $\mathbf{q}$, $\hat{\mathbf{n}}$ the unit vector in the z direction, and $\hat{\mathbf{t}}$ the in-plane vector perpendicular to $\hat{\mathbf{q}}$ and $\hat{\mathbf{n}}$. These vectors are expressed in the Cartesian basis $(\mathbf{e}_x, \mathbf{e}_y, \mathbf{e}_z)$ as

$$\hat{\mathbf{q}} = \frac{q_x}{q}\mathbf{e}_x + \frac{q_y}{q}\mathbf{e}_y,$$

$$\hat{\mathbf{t}} = \frac{q_y}{q}\mathbf{e}_x - \frac{q_x}{q}\mathbf{e}_y,$$

$$\hat{\mathbf{n}} = \mathbf{e}_z. \tag{6}$$

The velocity and the force are written as $\mathbf{v}=v_l\hat{\mathbf{q}}+v_t\hat{\mathbf{t}}+v_z\hat{\mathbf{n}}$ and $\mathbf{F}=F_l\hat{\mathbf{q}}+F_t\hat{\mathbf{t}}+F_z\hat{\mathbf{n}}$, respectively. Inserting these representations into the Stokes equations (1) and (2) finally leads to a system of ordinary differential equations for the Fourier-transformed quantities,

$$-\eta_\alpha q^2 \tilde{v}_l + \eta_\alpha \frac{\partial^2 \tilde{v}_l}{\partial z^2} - iq\tilde{p} + \tilde{F}_l \delta(z - z_0) = 0, \tag{7}$$

$$-\eta_\alpha q^2 \tilde{v}_t + \eta_\alpha \frac{\partial^2 \tilde{v}_t}{\partial z^2} + \tilde{F}_t \delta(z - z_0) = 0, \tag{8}$$

$$-\eta_\alpha q^2 \tilde{v}_z + \eta_\alpha \frac{\partial^2 \tilde{v}_z}{\partial z^2} - \frac{\partial \tilde{p}}{\partial z} + \tilde{F}_z \delta(z - z_0) = 0, \tag{9}$$

with the divergenceless condition

$$iq\tilde{v}_l + \frac{\partial \tilde{v}_z}{\partial z} = 0. \tag{10}$$

Although this framework is not as transparent as the usual image method, its advantages are twofold. On the one hand, it is particularly well suited to accommodate the description of the interface energy in Fourier space, since it thoroughly accounts for the symmetries of the problem. On the other hand, the transverse component of the velocity is decoupled from the longitudinal and normal directions. Moreover, relation (10) provides a useful link between $\tilde{v}_l$ and $\tilde{v}_z$, so that it is not difficult to get a single, fourth-order differential equation for the normal component only,

$$\frac{\partial^4 \tilde{v}_z}{\partial z^4} - 2q^2 \frac{\partial^2 \tilde{v}_z}{\partial z^2} + q^4 \tilde{v}_z = \frac{q^2 \tilde{F}_z}{\eta_1}\delta(z - z_0) + \frac{iq\tilde{F}_l}{\eta_1}\delta'(z - z_0). \tag{11}$$

Here, δ' is the derivative of the delta function.

D. Boundary conditions

To describe the flow in the presence of an interface, we must consider the flow on each side separately, and then require proper matching conditions for the velocity and surface forces. The hypothesis of smooth deformations around the planar configuration enables us to reformulate the problem in terms of equivalent boundary conditions at the undisplaced interface $z=0$ [20]. The appropriate conditions are (i) the continuity of the velocity, (ii) the continuity of tangential constraints, and (iii) the discontinuity of normal forces. Because the representation of the velocity in terms of longitudinal and transverse coordinates is not commonly used in the literature, we find it worthwhile to give in Appendix A some details regarding the derivation of the boundary values.

We finally assume that the two fluids are immiscible, a condition that is also enforced at height $z=0$. This approximation is justified since the fact that it is at any rigor valid at $z=h$ is an effect of higher order. Within this assumption, the time rate of change of the shape function is related to the normal velocity at the interface through

$$\tilde{v}_z(\mathbf{q}, 0, \omega) = i\omega\tilde{h}(\mathbf{q}, \omega), \tag{12}$$

up to linear order in the deformation field. This closure relation is especially relevant since, as shown in the following, it allows us to work out the instantaneous deformation of the interface in response to hydrodynamic stresses.

III. GREEN'S FUNCTION AND TRANSLATIONAL MOBILITY

A. Motion of the interface

We now have all the ingredients to solve the Stokes equations. Because the calculations are algebraically involved, we save the details for the Appendixes. Because of the linearity of the problem, the local deformation of the interface is directly proportional to the amplitude of the point force applied at height z_0,

$$\tilde{h}(\mathbf{q}, \omega) = \tilde{\mathbf{R}}(\mathbf{q}, z_0, \omega) \cdot \tilde{\mathbf{F}}(\omega), \tag{13}$$

where the vector $\tilde{\mathbf{R}}$ is the response function obtained thanks to the closure relation (12). For a vertical force $\tilde{\mathbf{F}} = (0, 0, \tilde{F}_z)$, we find in Appendix B

$$\tilde{R}_z(\mathbf{q}, z_0, \omega) = \frac{1}{4\bar{\eta}q(\omega_q + i\omega)}(1 + qz_0)e^{-qz_0}. \tag{14}$$

As expected, the relaxation dynamics of the profile is governed by the *mean* viscosity $\bar{\eta}=(\eta_1+\eta_2)/2$. The response of a deformation mode with wave vector $\mathbf{q}$ is characterized by its relaxation rate

$$\omega_q = \frac{\gamma}{4q\bar{\eta}}(q^2 + l_c^{-2}). \tag{15}$$

we remark that different wave vectors are not damped in the same way. The amplitude of the response function is always maximum for $\mathbf{q}=\mathbf{0}$, $\tilde{h}(\mathbf{0}, \omega)=\tilde{F}_z/(\Delta\rho g)$. It then vanishes with increasing q, all the more rapidly as the frequency ω or the distance z_0 becomes large. The real part of $\tilde{R}_z$, which is in phase with the strain, is the analog of a storage modulus for a viscoelastic medium [28]. This contribution corresponds to the elastic energy stored in the deformation of the interface. On the other hand, the imaginary part of $\tilde{R}_z$ plays the role of a loss modulus and describes the viscous dissipation associated with the relaxation of individual deformation modes.

The motion of the interface in real space is readily obtained from the inverse Fourier transform of the response

function, though the calculations will not be performed here. A deformation may also be obtained as a result of a point force applied parallel to the interface. We find

$$\tilde{R}_l(\mathbf{q},z_0,\omega)=\frac{1}{4\bar{\eta}q(\omega-i\omega_q)}qz_0e^{-qz_0}, \tag{16}$$

$$\tilde{R}_t(\mathbf{q},z_0,\omega)=0 \tag{17}$$

for the longitudinal and transverse coordinates, respectively. Note that the shape of the interface is not affected by the transverse component of the force.

B. Green's function

The components of the Green's function are then obtained by identification with the definition

$$\tilde{v}_i=\sum_j \tilde{\mathcal{G}}_{ij}\tilde{F}_j, \tag{18}$$

where $i,j\in\{l,t,z\}$. As shown in Appendix B, the Green's function can always be written as

$$\begin{aligned}\tilde{\mathcal{G}}(\mathbf{q},z,z_0,\omega)&=\tilde{\mathcal{G}}^{(0)}(\mathbf{q},z-z_0)+\Delta\tilde{\mathcal{G}}(\mathbf{q},z,z_0,\omega)\\&=\tilde{\mathcal{G}}^{(0)}(\mathbf{q},z-z_0)+\Delta\tilde{\mathcal{G}}^{(1)}(\mathbf{q},z,z_0)\\&\quad+\frac{\omega}{\omega-i\omega_q}\Delta\tilde{\mathcal{G}}^{(2)}(\mathbf{q},z,z_0)\end{aligned} \tag{19}$$

see Appendix B 1 for the exact expression of $\tilde{\mathcal{G}}_{tj}$, Appendix B 2 for the components $\tilde{\mathcal{G}}_{zj}$, and Appendix B 3 for the components $\tilde{\mathcal{G}}_{lj}$. The first term, which depends only the relative distance $(z-z_0)$, would reduce to the usual free-space Green's function if the viscosities were equal. The second term, $\Delta\tilde{\mathcal{G}}^{(1)}$, is the correction for an undistorted interface. Both contributions have already been obtained in previous work, though not in this particular choice of coordinates [18]. The original part of this study is the derivation of the contribution coming from the deformation of the interface, characterized by the prefactor $(\omega-i\omega_q)^{-1}$ in Eq. (19). This is a clear signature of hydrodynamic interactions with the soft surface. Note that the correction vanishes for $\gamma\to\infty$, and one recovers the results for the flat liquid-liquid interface in the high surface tension limit.

Finally, once all the components are known in the $(\hat{\mathbf{q}},\hat{\mathbf{t}},\hat{\mathbf{n}})$ basis, it is not difficult to express the Green's function in Cartesian coordinates. In particular, the diagonal components are given by

$$\tilde{\mathcal{G}}_{xx}=\frac{q_x^2}{q^2}\tilde{\mathcal{G}}_{ll}+\frac{q_y^2}{q^2}\tilde{\mathcal{G}}_{tt}, \tag{20}$$

$$\tilde{\mathcal{G}}_{yy}=\frac{q_y^2}{q^2}\tilde{\mathcal{G}}_{ll}+\frac{q_x^2}{q^2}\tilde{\mathcal{G}}_{tt}. \tag{21}$$

Similar relations can be deduced for off-diagonal terms, though they will not be required in the following.

C. Translational mobility tensor

From the matrix elements of the Green's function, we can obtain the mobility matrix for a sphere. With this aim, we still have to enforce the no-slip boundary condition for the fluid flow on the surface of the particle. In the following, we assume that the particle is a sphere of radius a. If we denote by $\mathbf{U}(\mathbf{r}_0)$ and $\mathbf{\Omega}$, respectively, the translational and rotational velocity of the sphere, $\mathbf{r}_0$ being the position of its center of mass, then the fluid velocity satisfies

$$\mathbf{v}(\mathbf{r}_0+\mathbf{a})=\mathbf{U}(\mathbf{r}_0)+\mathbf{\Omega}\times\mathbf{a}, \tag{22}$$

for any vector $\mathbf{a}$ scanning the surface of the bead. Integrating the total force over the surface of the particle together with the no-slip condition, one obtains a linear relation between the friction force $\mathbf{F}_H$ exerted by the liquid and velocity of the particle [22]. This relation defines the (frequency-dependent) mobility tensor through $\tilde{\mathbf{U}}=-\tilde{\mu}\tilde{\mathbf{F}}_H$. It can be written as the sum of two terms $\tilde{\mu}_{kl}(z_0,\omega)=\mu_0\delta_{kl}+\Delta\tilde{\mu}_{kl}(z_0,\omega)$, with $\mu_0=(6\pi\eta_1 a)^{-1}$ the bulk value for a particle in fluid 1 but infinitely far from the interface. The correction $\Delta\tilde{\mu}_{kl}$ is then expanded in powers of a/z_0. In the limit of small particles $a\ll z_0$, the correction to the mobility tensor is given, at leading order, by

$$\Delta\tilde{\mu}_{kl}(z_0,\omega)=\int\frac{d^2\mathbf{q}}{(2\pi)^2}\Delta\tilde{\mathcal{G}}_{kl}(\mathbf{q},z_0,z_0,\omega). \tag{23}$$

As a matter of fact, all cross contributions vanish because of reflection symmetry, and the rotational symmetry implies $\Delta\tilde{\mu}_{xx}=\Delta\tilde{\mu}_{yy}$. Thus, the correction to the mobility tensor is also diagonal with elements $\Delta\tilde{\mu}_{xx}=\Delta\tilde{\mu}_{yy}=\Delta\tilde{\mu}_{\parallel}$ and $\Delta\tilde{\mu}_{zz}=\Delta\tilde{\mu}_{\perp}$.

1. Perpendicular mobility

From the result Eq. (B11) for the normal-normal component of the Green's function, we find

$$\Delta\tilde{\mu}_{\perp}(z_0,\omega)=-\frac{1}{16\pi\eta_1 z_0}\left(\frac{2\eta_1+3\eta_2}{\eta_1+\eta_2}\right)+\frac{5}{32\pi\bar{\eta}z_0}F\left(\omega\tau,\frac{z_0}{l_c}\right). \tag{24}$$

In this expression, $\tau=4\bar{\eta}l_c/\gamma$ corresponds to the longest time required for elastic structures in the fluid—in our case, the interface—to relax. For typical values $\bar{\eta}=10^{-2}$ Pa s and $\Delta\rho=10^2$ kg m^{-3}, it ranges from $\tau\approx10^{-3}$ s for the usual interfaces with $\gamma=100$ mN m^{-1} up to $\tau\approx1$ s for ultrasoft interfaces with $\gamma=0.1$ μN m^{-1} [24]. The frequency-dependent contribution F arises from surface deformations and is therefore governed by the mean viscosity $\bar{\eta}$. It is given by

$$\begin{aligned}F(s,k)&=\frac{4}{5}\int_0^\infty dx\frac{iksx}{1+isx+x^2}(1+kx)^2\exp(-2kx)\\&=F'(s,k)+iF''(s,k).\end{aligned} \tag{25}$$

This integral actually corresponds to the sum over all deformation modes of the interface [29]. For $\omega=0$, one has $F(0,z_0/l_c)=0$ and the knowledgeable reader will recognize on the right-hand side of Eq. (24) the correction to the mo-

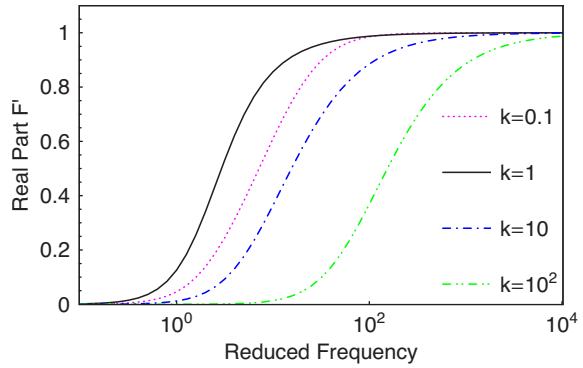

FIG. 1. (Color online) Real part F' as a function of the reduced frequency $s=\omega\tau$, for different values of the reduced distance $k=z_0/l_c$. The position of the crossover between the two regimes $\omega\tau \ll 1$ and $\omega\tau \gg 1$ is quite sensitive to the distance to the interface.

bility of a sphere near a flat, liquid-liquid interface [18]. One even recovers the result of Lorentz for a hard wall by taking the limit $\eta_2 \to \infty$ [1]. For finite values of ω, the additional term is actually a complex number. Its real part F' represents the contribution to the viscous dissipation that comes from interface deformations. As shown in Fig. 1, F' is positive for any value of the parameters, so that the real part of the mobility increases when the constraint on the shape of the interface is released. Viscous dissipation is therefore always lower for a soft interface, which can bend under hydrodynamic forces, than for a rigid interface.

Another outcome of Eq. (25) is that the mobility of the particle also exhibits an imaginary part F'', which corresponds to the storage of elastic energy in the deformation of the interface. As shown in Fig. 2, F'' is nonzero only for intermediate values of the frequency $\omega\tau \sim 1$. The latter contribution vanishes when $\omega \to \infty$ and one gets in this limit

$$\Delta\tilde{\mu}_\perp(z_0, \omega \to \infty) = \frac{3}{16\pi\eta_1 z_0}\left(\frac{\eta_1 - \eta_2}{\eta_1 + \eta_2}\right). \tag{26}$$

Lastly, we remark from Figs. 1 and 2 that both F' and F'' are of $O(1)$ for a wide range of reduced distances z_0/l_c. But

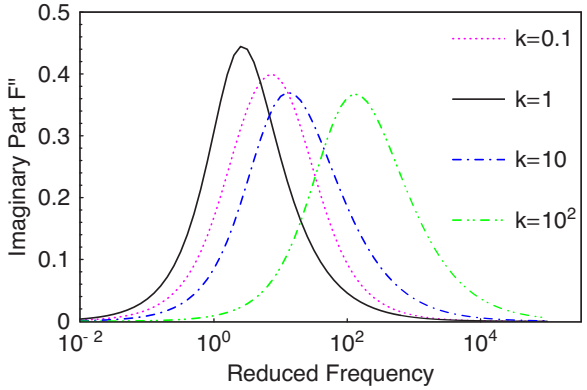

FIG. 2. (Color online) Imaginary part F'' as a function of the reduced frequency $s=\omega\tau$, for different values of the reduced distance $k=z_0/l_c$. The elastic coupling is maximum around the value $\omega\tau \sim 1$.

because of the prefactor z_0^{-1} in Eq. (24), the coupling between the motion of the particle and the shape of the interface vanishes when the particle is far away from the surface, as one might expect.

2. Parallel mobility

Similar conclusions can be drawn for the mobility parallel to the surface. Explicitly, we find

$$\Delta\tilde{\mu}_\parallel(z_0, \omega) = \frac{1}{32\pi\eta_1 z_0}\left(\frac{2\eta_1 - 3\eta_2}{\eta_1 + \eta_2}\right) + \frac{1}{64\pi\bar{\eta}z_0} G\left(\omega\tau, \frac{z_0}{l_c}\right), \tag{27}$$

where the frequency-dependent contribution is given by

$$G(s,k) = 4\int_0^\infty dx \frac{iksx}{1 + isx + x^2} k^2 x^2 \exp(-2kx). \tag{28}$$

In particular, one recovers the mobility coefficient for a sphere near a rigid interface in the asymptotic limit $\omega\tau \ll 1$,

$$\Delta\tilde{\mu}_\parallel(z_0, \omega = 0) = \frac{1}{32\pi\eta_1 z_0}\left(\frac{2\eta_1 - 3\eta_2}{\eta_1 + \eta_2}\right), \tag{29}$$

whereas one obtains in the other limit $\omega\tau \gg 1$,

$$\Delta\tilde{\mu}_\parallel(z_0, \omega \to \infty) = \frac{3}{32\pi\eta_1 z_0}\left(\frac{\eta_1 - \eta_2}{\eta_1 + \eta_2}\right). \tag{30}$$

3. Interpretation of the results

Equations (24), (25), (27), and (28) are the main outcome of this paper and deserve a few comments. With this aim, let us focus on the relaxation time of the interface, $\tau = 4\bar{\eta}l_c/\gamma \propto 1/\sqrt{\gamma}$. As recently suggested in the context of fluid membranes [19], the asymptotic behaviors of the mobility coefficient can be understood from this definition.

(1) It can be readily noticed that the limit $\omega\tau \ll 1$ actually coincides with the limit $\gamma \to \infty$. At very low frequencies, the interface thus appears infinitely rigid and one therefore recovers the well-known mobility coefficient of a particle near a flat, liquid-liquid interface [18].

(2) A similar reasoning applies to the limit $\omega\tau \gg 1$. For high frequency oscillations, the particle experiences an interface between two liquids with vanishing surface tension. As a consequence, the corrections have to cancel out if $\eta_1 = \eta_2$—see Eqs. (26) and (30).

The asymptotic behaviors of F' directly follow from these two points. Regarding F'', it is clear that elastic deformation energy can be stored neither in an infinitely rigid interface ($\gamma \to \infty$), nor in an infinitely soft interface ($\gamma \to 0$). This explains why this contribution vanishes at both low and high frequency.

Finally, notice that the sign of the real part of $\Delta\tilde{\mu}_\perp$ may change depending on whether $\omega\tau \ll 1$ or $\omega\tau \gg 1$. Indeed, it is always negative at low frequencies, whereas it may be positive at high frequencies provided that $\eta_1 > \eta_2$. This behavior is unusual since the presence of a surface generally hinders the perpendicular motion of a particle. This property, peculiar to soft interfaces, may strongly influence the dynamic

properties of Brownian particles since surface deformation may enhance diffusion—with regard to the bulk value—at short times.

IV. DISCUSSION

To summarize, we have calculated the mobility tensor of a spherical particle moving close to a fluid-fluid interface. Several lengths are inherent in the system, namely, the radius a of the particle, the distance from the wall, z_0, and the capillary length l_c. The results presented in this work concern the response to a point force and are valid for particles far from the interface, $a \ll z_0$, and for small amplitude of the particle oscillations. Because a soft interface can deform and store elastic energy, the mobility tensor decomposes into a real and an imaginary part. In the steady-state limit $\omega\tau \ll 1$, deformations are irrelevant and one recovers the classical result for a flat, fluid-fluid interface. On the other hand, the short-time limit $\omega\tau \gg 1$ presents the intriguing feature that the perpendicular mobility can be higher than the bulk mobility if $\eta_1 > \eta_2$. Yet this result does not break any fundamental law since it arises from the fact that the particle experiences the other side of the interface, which has a lower shear viscosity. Finally, coming back to the time variable, the friction force experienced by the particle will be expressed as a convolution product and is therefore nonlocal in time. Solvent backflow and delay of the response of the elastic interface then induce memory effects in the motion of the particle.

The framework developed in this study may be adapted to various problems near soft interfaces. For instance, one might investigate surface-mediated contributions to the coupled diffusion of two particles. One can also consider more complex surfaces, such as surfactant-covered interfaces or fluid membranes. Predictions regarding the rotational mobility might be relevant for experiments as well, especially in the case of anisotropic particles. Note that translational and rotational motions are not coupled for a sphere in the linearized theory. This might no longer be true for large deformations, where nonlinear effects come into play [30].

Another point that might be included in the theory is the effect of fluid inertia. This contribution has been neglected so far, though it becomes relevant at frequencies higher than $\omega_c = \eta/(\rho a^2)$. For typical values $\eta = 10^{-3}$ Pa s, $\rho = 10^3$ kg m^{-3}, and $a = 1$ μm, we obtain $\omega_c \approx 10^6$ rad s^{-1}. Here, however, we consider time scales comparable to the relaxation time of the interface. This corresponds to frequencies in the kilohertz range, so that our approximation is fully justified. At this point, it should be mentioned that a study similar to ours, including fluid inertia, has recently been published [31]. The author considers an interface with nonzero dilatational and shear moduli E^S and G^S, and obtains in the steady limit the result for a rigid wall with stick boundary conditions. The origin of this discrepancy is likely due to the fact that we consider a system with $E^S = G^S = 0$, but a closer inspection would be required to elucidate this question.

Finally, let us briefly comment on some possible comparisons with experiments. Recently, de Villeneuve *et al.* considered the sedimentation of polymethyl methacrylate spheres toward an interface with ultralow tension $\gamma \approx 0.1$ μN/m [32]. In this regime, long-range hydrodynamic interactions are dominant and lubrication theory does not apply. The authors clearly observe strong deformations of the interface, of the order of several micrometers for spheres with radius $a = 15$ μm [32]. Moreover, they measure sedimentation velocities that do not follow the theoretical curves for an undistorted interface, the particles falling faster toward the soft interface. The interpretation of those results might be quite straightforward in the light of the present analysis, even though the nonlinear equations of motion might be challenging to solve. Work on this question is currently under progress.

ACKNOWLEDGMENTS

D. Aarts, L. Bocquet, I. Pagonabarraga, and V. de Villeneuve are gratefully acknowledged for useful discussions. The author also wishes to thank S. Villain-Guillot and A. Würger for most valuable comments.

APPENDIX A: BOUNDARY CONDITIONS

We give in this appendix some details regarding the derivation of the boundary values, expressed at the undisplaced interface $z = 0$.

1. Continuity of the velocity

First of all, we have to ensure that the velocity is continuous at the interface. Explicitly, this requirement reads

$$\tilde{v}_l(\mathbf{q}, 0^+, \omega) = \tilde{v}_l(\mathbf{q}, 0^-, \omega), \tag{A1}$$

$$\tilde{v}_t(\mathbf{q}, 0^+, \omega) = \tilde{v}_t(\mathbf{q}, 0^-, \omega), \tag{A2}$$

$$\tilde{v}_z(\mathbf{q}, 0^+, \omega) = \tilde{v}_z(\mathbf{q}, 0^-, \omega). \tag{A3}$$

Interestingly, the condition (A1) for the longitudinal coordinate together with the incompressibility condition (10) implies an additional boundary condition for the normal coordinate of the velocity, namely,

$$\left.\frac{\partial \tilde{v}_z}{\partial z}\right|_{0^+} = \left.\frac{\partial \tilde{v}_z}{\partial z}\right|_{0^-}. \tag{A4}$$

2. Balance of tangential forces

Secondly, tangential stresses have to be balanced at the interface. In real space, the continuity condition for the normal-tangential components of the stress tensor reads $\sigma_{zx}|_{0^+} = \sigma_{zx}|_{0^-}$ and $\sigma_{zy}|_{0^+} = \sigma_{zy}|_{0^-}$, with $\sigma_{jk} = -p\delta_{jk} + \eta_\alpha(\partial v_j/\partial x_k + \partial v_k/\partial x_j)$ the stress tensor in Cartesian coordinates. Switching to $\{\mathbf{q}, z, \omega\}$ variables, both requirements reduce to

$$\eta_1 \left(\frac{\partial \tilde{\mathbf{v}}_\parallel}{\partial z} + i\mathbf{q}\tilde{v}_z\right)\bigg|_{0^+} = \eta_2 \left(\frac{\partial \tilde{\mathbf{v}}_\parallel}{\partial z} + i\mathbf{q}\tilde{v}_z\right)\bigg|_{0^-},$$

where the two-dimensional vector $\tilde{\mathbf{v}}_\parallel = (\tilde{v}_l, \tilde{v}_t)$ is the parallel velocity. Projecting this equation onto the transverse direction leads to the condition

$$\eta_1 \left.\frac{\partial \tilde{v}_t}{\partial z}\right|_{0^+} = \eta_2 \left.\frac{\partial \tilde{v}_t}{\partial z}\right|_{0^-}, \tag{A5}$$

whereas projection onto the longitudinal coordinate gives another condition which still involves both $\tilde{v}_l$ and $\tilde{v}_z$. In order to obtain a boundary condition for the normal component only, the incompressibility condition (10) is once more invoked. We finally get

$$\eta_1 \left.\left(\frac{\partial^2 \tilde{v}_z}{\partial z^2} + q^2 \tilde{v}_z\right)\right|_{0^+} = \eta_2 \left.\left(\frac{\partial^2 \tilde{v}_z}{\partial z^2} + q^2 \tilde{v}_z\right)\right|_{0^-}. \tag{A6}$$

Note that the balance of tangential stresses is also relevant with regard to the normal component of the velocity.

3. Discontinuity of normal stress

The next condition that has to be enforced concerns the normal-normal stress difference that comes into play whenever the interface is bent. Indeed, a deformation of the interface gives rise to normal restoring forces, expressed as the functional derivative of the Hamiltonian (4). For small displacements, the forces are small and proportional to h. The normal stress condition reads, in real space, $\sigma_{zz}|_{0^-} - \sigma_{zz}|_{0^+} = -\delta\mathcal{H}/\delta h$. In terms of the variables $\{\mathbf{q}, z, \omega\}$, we have

$$\tilde{p}(0^+) - \tilde{p}(0^-) - 2\eta_1 \left.\frac{\partial \tilde{v}_z}{\partial z}\right|_{0^+} + 2\eta_2 \left.\frac{\partial \tilde{v}_z}{\partial z}\right|_{0^-} = -E_q \tilde{h}(\mathbf{q}, \omega),$$

where we define the energy density $E_q = \gamma(q^2 + \lambda^{-2})$. It can be seen that the normal stress difference at the interface is balanced by interfacial tension and buoyancy forces (due to the density difference between the two fluids). This condition still involves both the normal component of the velocity as well as the pressure field. To get a relation in terms of $\tilde{v}_z$ only, we shall first use Eq. (7) to express the pressure difference (remember that $z_0 > 0$)

$$iq(\tilde{p}(0^+) - \tilde{p}(0^-)) = \eta_1 \left.\left(\frac{\partial^2 \tilde{v}_l}{\partial z^2} - q^2 \tilde{v}_l\right)\right|_{0^+} - \eta_2 \left.\left(\frac{\partial^2 \tilde{v}_l}{\partial z^2} - q^2 \tilde{v}_l\right)\right|_{0^-}.$$

Substituting $\tilde{v}_l$, for $\tilde{v}_z$, thanks to relation (10), we arrive at the condition on the third derivative of the velocity

$$\eta_1 \left.\left(\frac{\partial^3 \tilde{v}_z}{\partial z^3} - 3q^2 \frac{\partial \tilde{v}_z}{\partial z}\right)\right|_{0^+} - \eta_2 \left.\left(\frac{\partial^3 \tilde{v}_z}{\partial z^3} - 3q^2 \frac{\partial \tilde{v}_z}{\partial z}\right)\right|_{0^-} = -q^2 E_q \tilde{h}(\mathbf{q}, \omega). \tag{A7}$$

APPENDIX B: SOLUTION OF THE STOKES EQUATIONS

1. Transverse component of the velocity

We begin with Eq. (8) for the transverse component, which is easier to solve since it does not couple with the longitudinal and vertical coordinates of the velocity. This equation can be rewritten as

$$\frac{\partial^2 \tilde{v}_t}{\partial z^2} - q^2 \tilde{v}_t = -\frac{\tilde{F}_t}{\eta_1 q^2} \delta(z - z_0). \tag{B1}$$

With the condition that the fluid is at rest at infinity, the solution is

$$\tilde{v}_t(\mathbf{q}, z, \omega) = \begin{cases} Ae^{-qz} & \text{for } 0 < z_0 < z, \\ Be^{qz} + Ce^{-qz} & \text{for } 0 < z < z_0, \\ De^{qz} & \text{for } z < 0 < z_0. \end{cases}$$

We then need to specify the boundary conditions in order to determine the four integration constants. The continuity of the velocity and the balance of tangential stresses at height $z=0$ give the conditions (A2) and (A5). We get another couple of conditions by invoking the standard continuity conditions for the Green's function at the singularity $z=z_0$. Explicitly, these requirements read

$$\tilde{v}_t(\mathbf{q}, z_0^+, \omega) = \tilde{v}_t(\mathbf{q}, z_0^-, \omega), \tag{B2}$$

$$\left.\frac{\partial \tilde{v}_t}{\partial z}\right|_{z_0^+} - \left.\frac{\partial \tilde{v}_t}{\partial z}\right|_{z_0^-} = -\frac{\tilde{F}_t}{\eta_1 q^2}. \tag{B3}$$

Enforcing the boundary conditions (A2), (A5), (B2), and (B3), we find the following expression for $z \geqslant 0$:

$$\tilde{v}_t(\mathbf{q}, z, \omega) = \frac{\tilde{F}_t}{2\eta_1 q}\left[e^{-q|z-z_0|} - \left(\frac{1-\lambda}{1+\lambda}\right)e^{-q(z+z_0)}\right], \tag{B4}$$

and for $z \leqslant 0$

$$\tilde{v}_t(\mathbf{q}, z, \omega) = \frac{\tilde{F}_t}{2\eta_2 q}\left(\frac{2}{1+\lambda}\right)e^{-q|z-z_0|}. \tag{B5}$$

The transverse components are then obtained by comparison of Eq. (B4) (for $z \geqslant 0$) or (B5) (for $z \leqslant 0$) with the definition of the Green's function $\tilde{v}_t = \tilde{\mathcal{G}}_{tl}\tilde{F}_l + \tilde{\mathcal{G}}_{tt}\tilde{F}_t + \tilde{\mathcal{G}}_{tz}\tilde{F}_z$. Obviously, we get $\tilde{\mathcal{G}}_{tl} = \tilde{\mathcal{G}}_{tz} = 0$, the only nonzero component being $\tilde{\mathcal{G}}_{tt}$. Note that the transverse component of the velocity is not affected by the shape of the interface.

2. Normal component of the velocity

a. Differential equation and general solution

A priori, the normal and the longitudinal components of the velocity are coupled with each other. But, since the relations (7), (9), and (10) relating $\tilde{p}$, $\tilde{v}_l$, and $\tilde{v}_z$ are linear, it is not difficult to get a single equation for $\tilde{v}_z$,

$$\frac{\partial^4 \tilde{v}_z}{\partial z^4} - 2q^2 \frac{\partial^2 \tilde{v}_z}{\partial z^2} + q^4 \tilde{v}_z = \frac{q^2 \tilde{F}_z}{\eta_1}\delta(z - z_0) + \frac{iq\tilde{F}_l}{\eta_1}\delta'(z - z_0), \tag{B6}$$

with δ' the derivative of the delta function. The solution of this fourth-order differential equation is then

$$\tilde{v}_z(\mathbf{q},z,\omega)=\begin{cases}(A+Bz)e^{-qz} & \text{for } z>z_0,\\ (C+Dz)e^{qz}+(E+Fz)e^{-qz} & \text{for } z<z_0,\\ (G+Hz)e^{qz} & \text{for } z<0.\end{cases}$$

For the sake of simplicity, we shall focus separately on the situations where ($\tilde{F}_l=0$, $\tilde{F}_z\neq 0$) and ($\tilde{F}_l\neq 0$, $\tilde{F}_z=0$). According to the superposition principle, each solution leads by identification to the components of the Green tensor $\tilde{\mathcal{G}}_{zz}$ and $\tilde{\mathcal{G}}_{zl}$, respectively. Obviously, the normal-transverse component is identically zero, $\tilde{\mathcal{G}}_{zt}=0$.

b. Normal-normal component

We first consider the case where $\tilde{F}_l=0$ and $\tilde{F}_z\neq 0$. In addition to the boundary conditions (A3), (A4), (A6), and (A7), we have to enforce the usual conditions for the Green's function at the singularity position $z=z_0$, namely, the velocity and its first and its second derivatives are continuous at $z=z_0$. The only discontinuity comes from the third derivative,

$$\left.\frac{\partial^3\tilde{v}_z}{\partial z^3}\right|_{z_0^+}-\left.\frac{\partial^3\tilde{v}_z}{\partial z^3}\right|_{z_0^-}=\frac{q^2\tilde{F}_z}{\eta_1}. \tag{B7}$$

The algebra involved to evaluate the height integration constants is rather lengthy but presents no difficulty. We simply give the resulting velocity field:

$$\tilde{v}_z(\mathbf{q},z,\omega)=\frac{\tilde{F}_z}{4\eta_1 q}\left[(1+q|z-z_0|)e^{-q|z-z_0|}-\left(\frac{1-\lambda}{1+\lambda}\right)[1+q(z+z_0)+2q^2zz_0]e^{-q(z+z_0)}\right]-\omega_q\tilde{h}(\mathbf{q},\omega)(1+qz)e^{-qz} \tag{B8}$$

for $z\geqslant 0$, and

$$\tilde{v}_z(\mathbf{q},z,\omega)=\frac{\tilde{F}_z}{4\eta_2 q}\left(\frac{2}{1+\lambda}\right)[1+q(z_0-z)]e^{q(z-z_0)}-\omega_q\tilde{h}(\mathbf{q},\omega)(1-qz)e^{qz} \tag{B9}$$

for $z\leqslant 0$. The velocity field still depends on the deformation of the interface, which itself is a function of the velocity through the closure relation (12). Evaluating the velocity (B8) or (B9) at height $z=0$ and comparing with (12) then leads to

$$\tilde{h}(\mathbf{q},\omega)=\frac{1}{\omega_q+i\omega}(1+qz_0)e^{-qz_0}\frac{\tilde{F}_z}{4\bar{\eta}q}. \tag{B10}$$

Bringing Eqs. (B8) and (B9) together with Eq. (B10), we finally obtain the normal-normal component of the Green's function:

$$\tilde{\mathcal{G}}_{zz}(\mathbf{q},z,z_0,\omega)=\frac{1}{4\eta_1 q}\left[(1+q|z-z_0|)e^{-q|z-z_0|}-\left(1+q(z+z_0)+\frac{2q^2zz_0}{1+\lambda}\right)e^{-q(z+z_0)}\right]+\frac{1}{4\bar{\eta}q}\frac{\omega}{\omega-i\omega_q}(1+qz)(1+qz_0)e^{-q(z+z_0)} \tag{B11}$$

for $z\geqslant 0$, and

$$\tilde{\mathcal{G}}_{zz}(\mathbf{q},z,z_0,\omega)=\frac{1}{4\eta_2 q}\left(\frac{2}{1+\lambda}\right)q^2zz_0e^{q(z-z_0)}+\frac{1}{4\bar{\eta}q}\frac{\omega}{\omega-i\omega_q}(1-qz)(1+qz_0)e^{q(z-z_0)} \tag{B12}$$

for $z\leqslant 0$.

c. Normal-longitudinal component

In order to get the component $\tilde{\mathcal{G}}_{nl}$ of the Green's function, we perform the same analysis expect that we now keep $\tilde{F}_l\neq 0$, whereas we set $\tilde{F}_z=0$. This time, the discontinuity imposed by δ' in Eq. (B6) has an effect on the second derivative of the velocity at $z=z_0$,

$$\left.\frac{\partial^2\tilde{v}_z}{\partial z^2}\right|_{z_0^+}-\left.\frac{\partial^2\tilde{v}_z}{\partial z^2}\right|_{z_0^-}=\frac{iq\tilde{F}_l}{\eta_1}, \tag{B13}$$

the velocity and its first and it third derivatives being continuous. The algebra being quite similar to that of the previous section, we shall skip the details. Once again, the velocity field depends on the deformation of the interface. Interestingly, a point force exerted parallel to the surface is responsible for a normal displacement of the fluid-fluid interface. Evaluating the velocity at height $z=0$ leads to the result

$$\tilde{h}(\mathbf{q},\omega)=\frac{1}{\omega-i\omega_q}qz_0e^{-qz_0}\frac{\tilde{F}_l}{4\bar{\eta}q}. \tag{B14}$$

Bringing everything together, we find the normal-longitudinal component of the Green's function

$$\tilde{\mathcal{G}}_{zl}(\mathbf{q},z,z_0,\omega)=\frac{i}{4\eta_1 q}\left[q(z_0-z)e^{-q|z-z_0|}+\left(\frac{1-\lambda}{1+\lambda}qz-qz_0-\frac{2q^2zz_0}{1+\lambda}\right)e^{-q(z+z_0)}\right]+\frac{i}{4\bar{\eta}q}\frac{\omega}{\omega-i\omega_q}(1+qz)qz_0e^{-q(z+z_0)} \tag{B15}$$

for $z\geqslant 0$, and

$$\tilde{\mathcal{G}}_{zl}(\mathbf{q},z,z_0,\omega) = -\frac{i}{4\eta_2 q}\left(\frac{2}{1+\lambda}\right)qz(1-qz_0)e^{q(z-z_0)} + \frac{i}{4\bar{\eta}q}\frac{\omega}{\omega-i\omega_q}(1-qz)qz_0e^{q(z-z_0)} \quad \text{(B16)}$$

for $z \leqslant 0$.

3. Longitudinal component of the velocity

To obtain the longitudinal component of the velocity, there is actually no need to solve the corresponding differential equation (7). Indeed, from the incompressibility condition (10), $\tilde{v}_l$ is related to $\tilde{v}_z$ thanks to $\tilde{v}_l=(i/q)\partial\tilde{v}_z/\partial z$. From the definition $\tilde{v}_l=\tilde{\mathcal{G}}_{ll}\tilde{F}_l+\tilde{\mathcal{G}}_{lz}\tilde{F}_z$ (since, of course, $\tilde{\mathcal{G}}_{lt}=0$), it is straightforward to get

$$\tilde{\mathcal{G}}_{ll}(\mathbf{q},z,z_0,\omega) = \frac{1}{4\eta_1 q}\left[(1-q|z-z_0|)e^{-q|z-z_0|} - \left(\frac{1-\lambda}{1+\lambda}\right)\left(1-q(z+z_0)+\frac{2q^2zz_0}{1-\lambda}\right)e^{-q(z+z_0)}\right] + \frac{1}{4\bar{\eta}q}\frac{\omega}{\omega-i\omega_q}q^2zz_0e^{-q(z+z_0)} \quad \text{(B17)}$$

for $z \geqslant 0$, and

$$\tilde{\mathcal{G}}_{ll}(\mathbf{q},z,z_0,\omega) = \frac{1}{4\eta_2 q}\left(\frac{2}{1+\lambda}\right)(1+qz)(1-qz_0)e^{q(z-z_0)} + \frac{1}{4\bar{\eta}q}\frac{\omega}{\omega-i\omega_q}q^2zz_0e^{q(z-z_0)} \quad \text{(B18)}$$

for $z \leqslant 0$. The longitudinal-normal component $\tilde{\mathcal{G}}_{lz}$ can be obtained following the same procedure, though it will not be required here.

[1] J. Happel and H. Brenner, *Low Reynolds Number Hydrodynamics* (Kluwer, Dordrecht, 1983).
[2] H. A. Lorentz, Abh. Theor. Phys. **1**, 23 (1907).
[3] K. H. Lan, N. Ostrowsky, and D. Sornette, Phys. Rev. Lett. **57**, 17 (1986).
[4] P. Holmqvist, J. K. G. Dhont, and P. R. Lang, Phys. Rev. E **74**, 021402 (2006).
[5] L. P. Faucheux and A. J. Libchaber, Phys. Rev. E **49**, 5158 (1994).
[6] A. Pralle, E.-L. Florin, E. H. K. Stelzer, and J. K. H. Hörber, Appl. Phys. A: Mater. Sci. Process. **66**, S71 (1998).
[7] E. R. Dufresne, T. M. Squires, M. P. Brenner, and D. G. Grier, Phys. Rev. Lett. **85**, 3317 (2000).
[8] B. Lin, J. Yu, and S. A. Rice, Phys. Rev. E **62**, 3909 (2000).
[9] F. Benmouna and D. Johannsmann, Eur. Phys. J. E **9**, 435 (2002).
[10] L. Joly, C. Ybert, and L. Bocquet, Phys. Rev. Lett. **96**, 046101 (2006).
[11] M. Joanicot and A. Ajdari, Science **309**, 887 (2005).
[12] C. Neto, D. R. Evans, E. Bonaccurso, H.-J. Butt, and V. S. J. Craig, Rep. Prog. Phys. **68**, 2859 (2005).
[13] E. Lauga and T. D. Squires, Phys. Fluids **17**, 103102 (2005).
[14] J. Blawzdziewicz, V. Cristini, and M. Loewenberg, Phys. Fluids **11**, 251 (1999).
[15] B. U. Felderhof, J. Chem. Phys. **124**, 124705 (2006).
[16] R. B. Jones, J. Chem. Phys. **121**, 483 (2004).
[17] B. U. Felderhof, J. Phys. Chem. B **109**, 21406 (2005).
[18] S. H. Lee, R. S. Chadwick, and L. G. Leal, J. Fluid Mech. **93**, 705 (1979).
[19] T. Bickel, Eur. Phys. J. E **20**, 379 (2006).
[20] S. H. Lee and L. G. Leal, J. Colloid Interface Sci. **87**, 81 (1982).
[21] For a recent overview, see S.-M. Yang and L. G. Leal, Int. J. Multiphase Flow **16**, 597 (1990).
[22] J. K. G. Dhont, *An Introduction to Dynamics of Colloids* (Elsevier, Amsterdam, 1996).
[23] S. A. Safran, *Statistical Thermodynamics of Surfaces, Interfaces, and Membranes* (Addison-Wesley, New York, 1994).
[24] D. G. A. L. Aarts, M. Schmidt, and H. N. W. Lekkerkerker, Science **304**, 847 (2004).
[25] H. Faxén, Ark. Mat., Astron. Fys. **17**, 27 (1923).
[26] U. Seifert, Adv. Phys. **46**, 13 (1997).
[27] S. Bhattacharya, J. Blawzdziewicz, and E. Wajnryb, Physica A **356**, 298 (2005).
[28] R. G. Larson, *The Structure and Rheology of Complex Fluids* (Oxford University Press, New York, 1999).
[29] As a matter of fact, the integral can be expressed in terms of sine integral and cosine integral functions, though the final result is quite complicated and not really more transparent than Eq. (25).
[30] C. Berdan II and L. G. Leal, J. Colloid Interface Sci. **87**, 62 (1982).
[31] B. U. Felderhof, J. Chem. Phys. **125**, 144718 (2006).
[32] V. W. A. de Villeneuve, D. G. A. L. Aarts, and H. N. W. Lekkerkerker, Colloids Surf., A **282**, 61 (2006).